Eur. Phys. J. D **9**, 283–287 (1999)

THE EUROPEAN PHYSICAL JOURNAL D
EDP Sciences
© Società Italiana di Fisica
Springer-Verlag 1999

Generation and electronic properties of lanthanide–cyclooctatetraene organometallic clusters in gas phase

T. Kurikawa, Y. Negishi, F. Hayakawa, S. Nagao, K. Miyajima, A. Nakajima, and K. Kaya[a]

Department of Chemistry, Faculty of Science and Technology, Keio University, 3-14-1 Hiyoshi, Kohoku-ku, Yokohama 223-8522, Japan

Received: 31 August 1998 / Received in final form: 5 November 1998

Abstract. Organometallic clusters of lanthanide (Ln = Nd, Er, Eu, and Yb) and 1,3,5,7-cyclooctatetraene (C_8H_8) were produced by a combination of laser vaporization and molecular beam methods. In the mass spectra of $[\mathrm{Ln}_n(C_8H_8)_m]$, compositions of $m = n + 1$ were magic numbers. From mass spectrometry, photoionization spectroscopy, and photoelectron spectroscopy, we have concluded that these magic-numbered clusters take multiple-decker sandwich structures in which Ln atoms and C_8H_8 molecules are alternatedly piled up. These sandwich clusters are formed through ionic bonds composed of multiply charged cations $[\mathrm{Ln}^{k+}$ ($k = 2$ and 3)] and multiply charged anions $[C_8H_8^{h-}$ ($h = 1$, 1.5, and 2)].

PACS. 36.40.-c Atomic and molecular clusters – 36.40.Mr Spectroscopy and geometrical structure of clusters – 61.46.+w Clusters, nanoparticles, and nanocrystalline materials – 71.24.+q Electronic structure of clusters and nanoparticles

1 Introduction

Since $U(C_8H_8)_2$ was discovered in 1968 [1], studies of organo-rare earth metal chemistry in a condensed phase have been an active area of experimental research. Specifically, questions regarding the degree of metal-ligand covalency have been addressed. It is now generally agreed that there is less involvement of f orbitals in lanthanide bonding than is generally assumed to operate in the actinides. Therefore, organolanthanide compounds have long been assumed to be optical, and magnetic materials for such $4f$ orbitals are shielded largely from external interactions by the outer $5s$ and $5p$ orbitals [2,3]. Numerous experimentalists and theoreticians have been prompted to describe the bonding of organolanthanide compounds as wholly ionic [4–7]. In the condensed phase, the alkali metal salts are generally prepared as $\mathrm{M}_{\mathrm{alkali}^+}[\mathrm{Ln}^{3+}(C_8H_8^{2-})_2]$. Similarly, divalent compounds of Eu and Yb can be described by ionic bonding, denoted as $(\mathrm{M}_{\mathrm{alkali}^+})_2[\mathrm{Ln}^{2+}(C_8H_8^{2-})_2]$. Because of such propensity, organolanthanide compounds have been apparently unsuitable for studies on neutral and multinuclear properties of the Ln–C_8H_8 system.

Our recent development of methodology combining a laser-vaporization method and a molecular beam method has opened up a new way for facile investigation of organometallic clusters [8,9]. In the gas phase, it is possible to understand a metal–molecule interaction without influence of the solvent. We have successfully produced organometallic lanthanide (Ln) and cyclooctatetraene (C_8H_8), $\mathrm{Ln}_n(C_8H_8)_m$, clusters from a mixture of vaporized metal atoms and aromatic molecules. The electronic and geometric structures of $\mathrm{Ln}_n(C_8H_8)_m$ were determined by mass spectrometry, photoionization spectroscopy, and photoelectron spectroscopy.

2 Experiment

$\mathrm{Ln}_n(C_8H_8)_m$ clusters [Ln = lanthanide metals of Nd, Er, Eu, and Yb; C_8H_8 = 1,3,5,7-cyclooctatetraene], were produced by the combination of the laser-vaporization method, the molecular beam method and a flow tube reactor (FTR) [10]. The experimental setup used in this work is described elsewhere [8,9]. First, Ln atoms were vaporized by a frequency doubled output from a Q-switched Nd^{3+}: YAG laser (532 nm, ∼ 10 mJ/pulse) and were cooled to room temperature with He carrier gas (5 atm stagnation pressure). After growth of the cluster in a channel (of 3 mm diameter and 4 cm length), C_8H_8 vapor (∼ 70 Torr; 70 °C) diluted with He carrier gas (1.5 atm) was synchronized with the flow of the metal vapor and was injected into the FTR. $\mathrm{Ln}_n(C_8H_8)_m$ binary clusters thus generated were sent into an ionization chamber through a skimmer (3 mm diameter). Then the clusters were ionized by an ArF excimer laser (193 nm; 6.42 eV) or a frequency doubled

---

[a] Corresponding author.

output of a tunable dye laser (310–209 nm; 4.00–5.92 eV) pumped by a XeCl excimer laser (308 nm) in a static electric field. The photoions were mass-analyzed by a reflectron time-of-flight (RETOF) mass spectrometer. To determine ionization energies (E_is), the frequency doubled output of the dye laser was used as the ionization light. Photon energy was changed at a 0.01–0.05 eV interval in the range of 5.92–3.90 eV, while the abundance and composition of $\mathrm{Ln}_n(\mathrm{C_8H_8})_m$ were monitored by the ionization of the ArF laser. Fluences of both the dye laser and the ArF laser were monitored by a pyroelectric detector (Molectron J-3) and were kept at $\sim 200\,\mu\mathrm{J/cm^2}$ to avoid multiphoton processes. To obtain photoionization efficiency (PIE) curves, ion intensities of the mass spectra were plotted as a function of photon energy with normalization to both the laser fluence and the ion intensities of the ArF mass spectra. The E_is of $\mathrm{Ln}_n(\mathrm{C_8H_8})_m$ were determined from the final decline of the PIE curves. Typical uncertainty of E_is is estimated to be ±0.05 eV.

To record photoelectron spectra, anion clusters were produced by the same procedure as in the case of neutral clusters. Then clusters produced were sent into an on-line TOF mass spectrometer by 3 keV for mass analysis and by 900 eV for a PES (photoelectron spectroscopy) study. After being decelerated, the mass-selected anions were photodetached with a fourth harmonic (266 nm, 4.66 eV) of the other $\mathrm{Nd^{3+}}$:YAG laser. The photoelectron signal was typically accumulated to 30 000 shots by a multichannel scaler/averager (Stanford Research System, SR430). Obtained energy resolution was about 70 meV FWHM at 1 eV electron energy. Energy of the photoelectron was calibrated by the measurement of photoelectron spectra of $\mathrm{Au^-}$ [11, 12]. The laser power for photodetachment was in the range of 10–20 $\mathrm{mJ/cm^2}$ for 355 nm and 1–3 $\mathrm{mJ/cm^2}$ for 266 nm and no power dependent processes for the spectrum shape were observed.

3 Results and discussion

3.1 Mass spectra of $\mathrm{Ln_n(C_8H_8)_m}$ clusters

Figures 1a–1d show typical examples of photoionization mass spectra of $\mathrm{Ln}_n(\mathrm{C_8H_8})_m$ [Ln = Nd, Er, Eu, and Yb] produced by the foregoing procedure. The peaks are labeled according to the notation (n, m), which denotes the number of Ln atoms (n) and $\mathrm{C_8H_8}$ molecules (m). In the photoionization mass spectra, the ion intensities would reflect the abundance of clusters when their E_is are lower than the photon energy of the ionization laser. Mass spectra of (n, m) clusters were measured under the condition of low fluence of the ionization lasers to prevent multiphoton ionization processes. Main peaks in the mass spectra were assigned as $\mathrm{Ln}_n(\mathrm{C_8H_8})_{n+1}$. In cationic mass spectra of $\mathrm{Ln}_n(\mathrm{C_8H_8})_m^+$, clusters having $m = n + 1$ were also observed as main products. Even when the concentration of $\mathrm{C_8H_8}$ vapor was changed to higher one, these main peaks remained unchanged. Therefore, these species are stable compositions under the condition. For bulk, DeKock *et al.* and Ely *et al.* reported a triple-decker sandwich cluster, $[(\mathrm{C_8H_8})\mathrm{Nd(THF)_2}][(\mathrm{C_8H_8})_2\mathrm{Nd}]$. Further, Greco *et al.* reported $\mathrm{Ce_2(C_8H_8)_3}$ [13–15]. By analogy with these findings, $\mathrm{Ln}_n(\mathrm{C_8H_8})_{n+1}$ clusters should take multiple-decker sandwich structures. Proposed structures of $\mathrm{Ln}_n(\mathrm{C_8H_8})_{n+1}$ clusters are shown in Fig. 3.

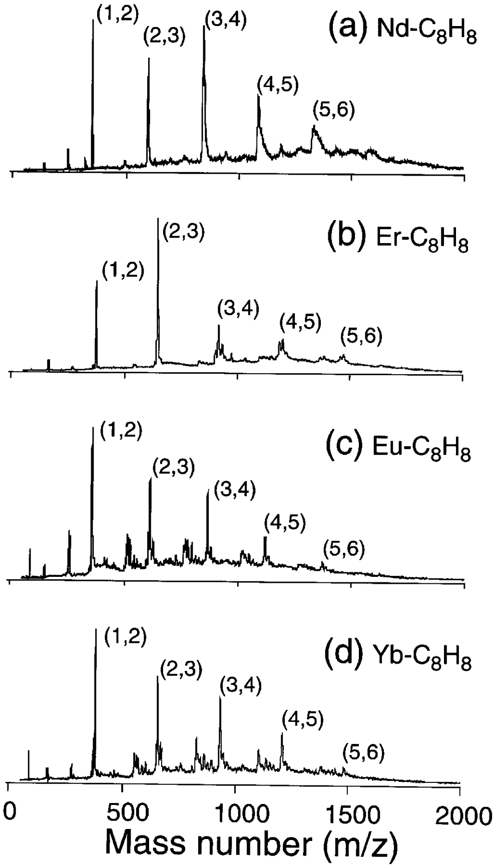

Fig. 1. Time-of-flight mass spectra of lanthanide (Ln)– 1,3,5,7-cyclooctatetraene ($\mathrm{C_8H_8}$) clusters, $\mathrm{Ln}_n(\mathrm{C_8H_8})_m$ [Ln = (a) Nd, (b) Er, (c) Eu, and (d) Yb] obtained by the photoionization of the ArF laser (6.42 eV). Peaks are labeled according to the notations (n, m), denoting the number of Ln atoms (n) and $\mathrm{C_8H_8}$ molecules (m). The intense peaks between magic-numbered clusters correspond to (n, n), (n, n)+oxide or (n, n)+water compositions. For Nd–$\mathrm{C_8H_8}$, mass peaks become broader with increasing mass due to many isotopes of Nd atoms.

3.2 PES spectra of $\mathrm{Ln(C_8H_8)_2^-}$ cluster anions

To elucidate further the bonding nature of these clusters, we conducted PES experiments for $\mathrm{Ln(C_8H_8)_2^-}$ anions at 266 nm (4.66 eV). The PES spectra are shown in Fig. 2. In the spectra, a horizontal axis corresponds to an electron binding energy, E_b, which is defined as $E_b = h\nu - E_k$ where E_k is a kinetic energy of the photoelectron and $h\nu$ is a photon energy of the photodetachment laser. To assign a photodetachment threshold energy, E_T, we linearly extrapolated the slope of the first onset to the baseline of the spectrum. A downward arrow indicates the E_T value

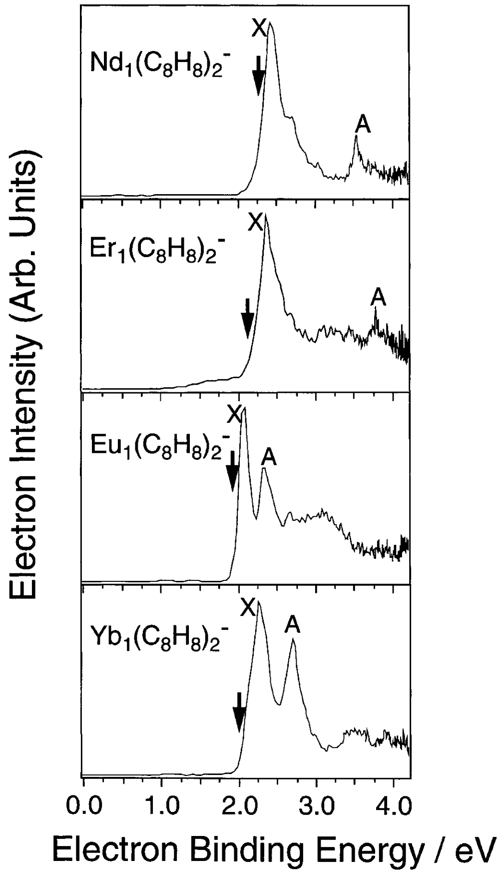

Fig. 2. Photoelectron spectra of $Ln(C_8H_8)_2{}^-$ anions (Ln = Nd, Er, Eu, and Yb) at 266 nm (4.66 eV). Arrows indicate threshold energies (E_T). The vertical detachment energy of each labeled peak is tabulated in Table 1.

Table 1. Threshold energies (E_T) and vertical detachment energies (VDE) of $Ln(C_8H_8)_2{}^-$ (/eV).

Ln	E_T		VDE
Nd	2.37(25)	X	2.43
		A	3.54
Er	2.06(16)	X	2.36
		A	3.76
Eu	2.02(09)	X	2.14
		A	2.68
Yb	1.95(10)	X	2.13
		A	2.65

Numbers in parentheses indicate experimental uncertainties; 2.37(25) represents 2.37 ± 0.25.

in each figure. The E_T values correspond to upper limits of adiabatic electron affinity (E_A). Besides the E_T values, vertical detachment energies (VDE) of the first peak are also derived from the peak maxima in the photoelectron spectra. E_T and VDE are tabulated in Table 1. When we look at the PES spectra, striking similarities can be seen. One is between Nd and Er, and the other is between Eu and Yb. In the former group, two peaks are located around the binding energy of 2.5 and 3.5 eV, and they have similar profiles, with a sharp leading edge and two shoulders on the higher binding energy side. In the latter one, first two sharp peaks are located around 2.0 and 2.5 eV, and they accompany weaker broad bands in the higher binding energy side. In bulk materials, these Ln elements are characterized as a highly ionic complex that depends on the oxidation state. Therefore, it is reasonable to assume that Nd and Er take the oxidation state of +3, while Eu and Yb take that of +2, by analogy to the reported lanthanide clusters.

As is well known because of the $4n+2$ rule of aromatics, a C_8H_8 molecule can act as an electron acceptor of 2 electrons. When the two-electron acceptability of C_8H_8 is considered in combination with the fact that $Ln(C_8H_8)_2$ in bulk materials have been prepared as potassium or lithium salts denoted as $M_{alkali^+}[Ln^{3+}(C_8H_8^{2-})_2]$ [16], it is rational to conclude that $Ln(C_8H_8)_2{}^-$ anions can be expressed as a $Ln^{3+}(C_8H_8^{2-})_2$ configuration for Nd and Er. In the configuration, each C_8H_8 molecule has 2 excess electrons. In the oxidation states of 3+, Nd^{3+} and Er^{3+} have 3 and 11 f electrons, respectively. As shown in their photoelectron spectra, this difference does not change the spectra. A PES experiment on neutral $Ce(C_8H_8)_2$ by Streitwieser *et al.* [17] suggests the assignment on photoelectron spectra of anionic $Nd(C_8H_8)_2{}^-$ and $Er(C_8H_8)_2{}^-$. They have proposed that the configuration of the neutral ground state of $Ce(C_8H_8)_2$ is $(a_{1g};\ 2C_8H_8)^2(a_{2u};\ 2C_8H_8)^2(e_{1g};\ 2C_8H_8)^4(e_{1u};\ 2C_8H_8)^4(e_{2g};\ 2C_8H_8)^4(e_{2u};\ 2C_8H_8)^3(e_{3u};\ Ce)^1$, and that the energy difference between $(e_{2g};\ 2C_8H_8)$ and $(e_{2u};\ 2C_8H_8)$ is about 0.93 eV. Since ground-state configuration of neutral $Ln^{4+}(C_8H_8^{2-})_2$ is unlikely from several theoretical calculations [18–20], we have assigned the configurations of the anion and the neutral ground states to be $Ln^{3+}(C_8H_8^{2-})_2$ $[(e_{2u};\ 2C_8H_8)^4(e_{3u};\ Ln)^k]$ and $Ln^{3+}(C_8H_8^{1.5-})_2$ $[(e_{2u};\ 2C_8H_8)^3(e_{3u};\ Ln)^k]$, respectively, where $k=3$ for Nd and $k=11$ for Er. Then, the plausible assignment is that the first peak of X corresponds to the photodetachment from the e_{2u} MO of C_8H_8, and that the second peak of A corresponds to that from the e_{2g} MO of C_8H_8; the symmetry of D_{8h} is assumed.

Eu and Yb are typical examples of stable Ln^{2+} complexes in bulk materials. This is because Eu and Yb possess $4f^7$ and $4f^{14}$ configurations in the oxidation states of +2, which correspond to the half-filled and fully-filled $4f$ orbitals, respectively, stabilized by the spin–spin exchange interaction. Therefore, their neutrals are considered to take $Eu^{2+}(C_8H_8^{1-})_2$ and $Yb^{2+}(C_8H_8^{1-})_2$ configurations. Differences between electronic and vibrational structures from Ln^{3+} clusters are ascribed to the change of electronic configuration of C_8H_8 from $(C_8H_8^{1.5-})_2$ to $(C_8H_8^{1-})_2$. In the photoelectron spectra, two strong bands were observed, and their gaps are 0.54 eV for neutral $Eu(C_8H_8)_2$ and 0.52 eV for neutral $Yb(C_8H_8)_2$. Based on the assignment for $Nd(C_8H_8)_2{}^-$ and $Er(C_8H_8)_2{}^-$, the two strong bands in $Eu(C_8H_8)_2{}^-$ and $Yb(C_8H_8)_2{}^-$ are assigned to those from e_{2u} and e_{2g}, respectively, although it seems that the neutral $Eu(C_8H_8)_2$ and $Yb(C_8H_8)_2$ have lower symmetry than D_{8h} that is due to deformation of the 8-membered

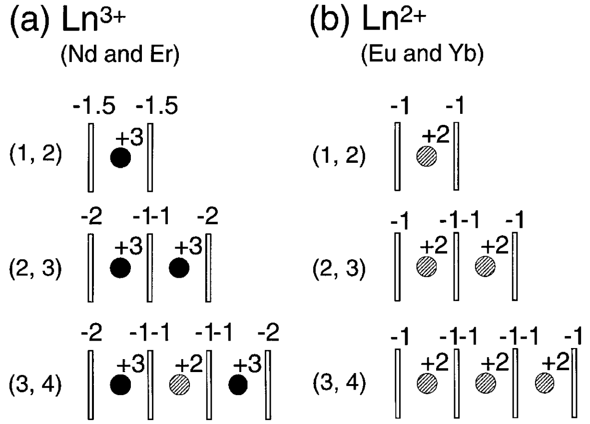

Fig. 3. Proposed structures and allotment of valence electrons of $Ln_n(C_8H_8)_{n+1}$ clusters: (a) Ln = Nd and Er; (b) Ln = Eu and Yb. These schematics are based on the assumption of two-electron acceptability of C_8H_8 and multiply charged positive ions of Ln (Ln^{3+} for Nd and Er, and Ln^{2+} for Eu and Yb). As shown in (a), one of the Ln atoms should become the +2 oxidation state in (3, 4); this results in low ionization energy.

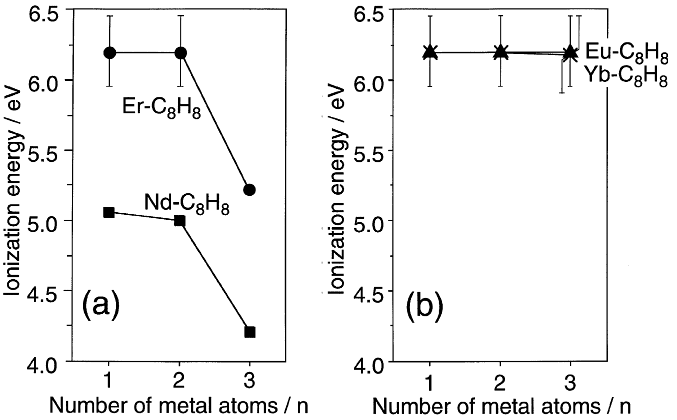

Fig. 4. Ionization energies (E_is) of multiple-decker sandwich clusters. (a) $Nd_n(C_8H_8)_{n+1}$ (solid square) and $Er_n(C_8H_8)_{n+1}$ (solid circle); (b) $Eu_n(C_8H_8)_{n+1}$ (solid triangle) and $Yb_n(C_8H_8)_{n+1}$ (cross lines). In the figures, the ionization energies contain large uncertainty, because the tunable dye laser has a limited emission range of at most 5.92 eV (209 nm).

ring of C_8H_8. Furthermore, the apparent broadening of these bands with the heavier lanthanide atoms is noticeable. Since there is no unpaired f electron in $Yb(C_8H_8)_2$, the broadening might be attributed not to the exchange interaction with the f electrons, but to the vibrational excitations of the ligand C_8H_8. In the high-energy side of the electron binding energy, broader bands were found 1 eV above the band X, and they might be contributed from the oxidation states of +3; the photodetachment from $Ln^{2+}(C_8H_8^{1.5-})_2$ to $Ln^{3+}(C_8H_8^{1.5-})_2$.

3.3 Ionization energies of neutral $Ln_n(C_8H_8)_{n+1}$

To determine the electronic properties of neutral $Ln_n(C_8H_8)_m$, we measured ionization energies (E_is) by using photoionization spectroscopy. The results were illustrated in Fig. 4. Several clusters in the figure contain large uncertainties of $5.92\,\text{eV} < E_i\text{s} < 6.42\,\text{eV}$, because the ionization energy of 5.92 eV corresponds to the maximum emission of the tunable dye laser. In Fig. 4, two patterns are easily conceivable. For $Nd_n(C_8H_8)_{n+1}$ and $Er_n(C_8H_8)_{n+1}$ (Fig. 4a), while E_is of $(1, 2)$ and $(2, 3)$ show similar values, E_is of $(3, 4)$ largely drop by 0.8 eV. For $Eu_n(C_8H_8)_{n+1}$ and $Yb_n(C_8H_8)_{n+1}$ (Fig. 4b), however, the E_i values are almost constant for $n = 1-3$, although the values have relatively large uncertainty. The two size dependences can be explained by the counting of valence electrons based on the multiply ionic states in the cluster. Considering that Ln atoms favor either Ln^{3+} or Ln^{2+} state in ligand field, allotment of valence electrons in multiple-decker $Ln_n(C_8H_8)_{n+1}$ should be as shown in Fig. 3. In case of Nd and Er, Ln atoms can exist as Ln^{3+} ions interposed by C_8H_8 for $n = 1$ and 2. For $n = 3$, however, one of Ln atoms in the multiple-decker structure cannot become an Ln^{3+} ion because of the lack of electron acceptability of C_8H_8. Then the Ln atom should result in a Ln^{2+} ion, as shown in Fig. 3a. E_is tends to drop at $(3, 4)$ for Ln = Nd and Er, but this can be reasonably explained by the change of valence electrons as follows: Since one of the Ln atoms in $(3, 4)$ should take the Ln^{2+} ion in the neutral ground state, large stabilization is expected for the cationic $(3, 4)+$, because of the change in charge from Ln^{2+} to Ln^{3+}. In $(1, 2)$ and $(2, 3)$, on the other hand, no cationic stability is expected, because the ionization process results in the one from Ln^{3+} to Ln^{4+}.

For all the Eu and Yb clusters, Eu and Yb atoms always take Ln^{2+} in the neutrals as shown in Fig. 3b. Rather high E_is of these clusters as compared to Ln atoms are ascribed to the stability of neutral clusters, in which Ln^{2+} atoms have half- and fully closed shell configuration. Since Nd atom ($4f^3$) in the cluster is an open-shell configuration in the neutral ground state, the E_is of $Nd_n(C_8H_8)_{n+1}$ were low compared to those of the Nd atoms ($E_i[\text{Nd}] = 5.49\,\text{eV}$). The fairly high E_is of $Er_n(C_8H_8)_{n+1}$ as compared to $Nd_n(C_8H_8)_{n+1}$ might be ascribed to the higher E_i of the Er atom (6.10 eV) than that of Nd atom.

In our previous report on multiple-decker sandwiches of $V_n(C_6H_6)_{n+1}$ ($n = 1-4$) [8], the E_is showed a drastic decrement as the cluster size increased. This phenomenon of E_i is theoretically elucidated by the fact that the ionization occurs from a delocalized molecular orbital of vanadium–vanadium interaction interposed by π^* orbitals of benzene [21]. In $Ln_n(C_8H_8)_{n+1}$, however, an orbital contributing to the ionization process is considered to be discontinuously localized along the molecular axis, because the cluster is bonded through ionic bonds and the charge is localized at each component. Since the first ionization is expected to occur from $4f$(Ln) orbitals in $(1, 2)$ [17, 22], we concluded that the $4f$ orbital in the cluster is localized and scarcely interacts with neighboring Ln atoms in the cluster. According to the theoretical calculation of Dolg and co-workers [18–20], $Nd(C_8H_8)_2$ is indeed a charge transfer cluster in which 3 of 6 electrons in $Nd(6s^24f^4)$ transfer almost completely to $2C_8H_8$, resulting in a configuration of $Nd^{3+}(C_8H_8^{1.5-})_2$. In case of Eu and Yb, the rather high E_is of $Eu_n(C_8H_8)_{n+1}$ and $Yb_n(C_8H_8)_{n+1}$ seem to ensure the complete charge transfer, because E_is of Eu and Yb clusters are rather high ($5.92\,\mathrm{eV} < E_i\mathrm{s} < 6.42\,\mathrm{eV}$) compared to Ln^{3+} clusters. We conclude from all the results that the bonding in $Ln_n(C_8H_8)_{n+1}$ is of ionic character, in which Ln atoms exist as multiply charged ions.

This work has been supported by the program "Research for the Future (RFTF)" of the Japan Society for the Promotion of Science (98P01203), and by a Grant-in-Aid for Scientific Research on Priority Areas from the Ministry of Education, Science, Sports, and Culture. T. K. expresses his gratitude to the Japan Society for the Promotion of Science for Young Scientists for a research fellowship.

References

1. A. Streitwieser, Jr., U. Müller-Westerhoff: J. Am. Chem. Soc. **90**, 7364 (1968)
2. J.V. Ortiz, R. Hoffmann: Inorg. Chem. **24**, 2095 (1985)
3. H. Rabaa, J.-Y. Saillard, R. Hoffmann: J. Am. Chem. Soc. **108**, 4327 (1986)
4. L.J. Nugent, P.G. Laubereau, G.K. Werner, K.L. Vander Sluis: J. Organomet. Chem. **27**, 365 (1971)
5. K.O. Hogson, F. Mares, D.F. Starks, A. Streitwieser, Jr.: J. Am. Chem. Soc. **95**, 8650 (1973)
6. K.N. Raymond, C.W. Eigenbrot: Acc. Chem. Res. **13**, 276 (1980)
7. R.A. Andersen, J.M. Bonsella, C.J. Burns, J.C. Green, D. Hohl, N. Rosch: J. Chem. Soc., Chem. Commun. 405 (1986)
8. K. Hoshino, T. Kurikawa, H. Takeda, A. Nakajima, K. Kaya: J. Phys. Chem. **99**, 3053 (1995)
9. T. Kurikawa, M. Hirano, H. Takeda, K. Yagi, K. Hoshino, A. Nakajima, K. Kaya: J. Phys. Chem. **99**, 16 248 (1995)
10. M.E. Geusic, M.D. Morse, S.C. O'Brien, R.E. Smalley: Rev. Sci. Instrum. **56**, 2123 (1985)
11. H. Hotop, W.C. Lineberger: J. Phys. Chem. Ref. Data **4**, 539 (1975)
12. V.A. Esulov: Ann. Phys. Fr. **11**, 493 (1986)
13. A. Greco, S. Cesca, G. Bertolini: J. Organomet. Chem. **113**, 321 (1976)
14. C.W. DeKock, S.R. Ely, T.E. Hopkins, M.A. Brault: Inorg. Chem. **17**, 625 (1978)
15. S.R. Ely, T.E. Hopkins, C.W. DeKock: J. Am. Chem. Soc. **98**, 1624 (1976)
16. K.O. Hodgson, K.N. Raymond: Inorg. Chem. **11**, 3030 (1972)
17. A. Streitwieser, Jr., S.A. Kinsley, J.T. Rigsbee: J. Am. Chem. Soc. **107**, 7786 (1985)
18. M. Dolg, P. Fulde, W. Küchle, C. Neumann, H. Stoll: J. Chem. Phys. **94**, 3011 (1991)
19. M. Dolg, P. Fulde, H. Stoll, H. Preuss, A. Chang, R.M. Pitzer: Chem. Phys. **195**, 71 (1995)
20. W. Liu, M. Dolg, P. Fulde: J. Chem. Phys. **107**, 3584 (1997)
21. T. Yasuike, S. Yabushita: J. Phys. Chem. A **103**, 4533 (1999)
22. J.P. Clark, J.C. Green: J. Chem. Soc., Dalton Trans. 505 (1977)